

The Effect of Bathymetry Changes on Meridional Overturning Currents

Marte Voorneveld
5911591

May 24, 2020

Abstract

1 Introduction

The geometry and resulting bathymetry of our planet is an ever changing phenomenon. In the last 120 Ma the earth moved from having one major oceanic system in the Pacific with a single large continent to the current 3 ocean system (Besse and Courtillot 2002). The Bathymetry changes that occurred in this time period are characterized by the opening and closing of certain passages through which exchange of water between the oceanic basins is observed. The exact timing of passage openings is a topic of rigorous debate in literature (Scher and Martin 2006, Schmidt 2007).

One of the changes on which there is general consensus, is the inception and expansion of the Atlantic ocean and the resulting decrease in size of the Pacific basin. The creation of the Atlantic basin has had major effects on the earth's climate, especially resulting in massive localized changes such as the temperate European climate, due to the north Atlantic meridional overturning current (AMOC). This creates the current Northern sinking oceanic throughflow in the Atlantic. However it is unknown when exactly this northern sinking started. With the past non-existance of the Atlantic it must have started some time in the last 40Ma with the advent of a larger Atlantic (Abelson and Erez 2017).

The result of these bathymetry changes on the oceanic stream function and the resulting overturning currents is something that has been previously studied by Mulder et al. 2017. They however found that using a Jacobian matrix for continuation in

each of the model years fails to simulate the onset of the Northern sinking AMOC that is physically observed. Here we instead propose to use a general circulation ocean model with only a changing bathymetry keeping the same initial forcing for each time step. This eliminates the need for a continuation using the Jacobian matrix method proposed in Mulder et al. 2017.

This paper will focus solely on changes in bathymetry using simplified zonally averaged global forcings. The results of the model will be used to estimate global changes in oceanic through flow at the critical passages. Furthermore the strength of the meridional overturning currents (MOC) will be studied.

2 Methods

2.1 Veros and Runtime

Ocean modeling has been an area of continued progress. The resolutions of the models have been steadily increasing since the inception of the first computerized ocean models. However, due to the age of some of these models and the continued adaptation of often old legacy Fortran code, many models have become enormous hurdles to get started with often resulting in frustration. The Veros ocean model project is trying to tackle this problem with a totally new code base written entirely in Python (**Hafner2018Aug**). Veros is a General Circulation Ocean model based on the suc-

cessful PyOm2 model. It was designed from the ground up with flexibility in mind. This flexibility cuts valuable time spent on figuring out the often cumbersome Fortran models of the past. Veros is specifically well suited for researching the effect of changes in both forcings and bathymetries. They can be easily edited using Python. These features in particular are heavily used in this paper. One of the most extensively used features for example is the fact that any bathymetry can, without further manual specifications of islands be used for stream function calculation.

In this case the models used in this paper are run on a 8 core (16 threads) machine using an MPI CPU configuration of 1 node.

2.2 Model Setup

2.2.1 Model Domain

The domain of the model is bounded by longitudes $\phi_E = -180^\circ$ and $\phi_W = 180^\circ$ and latitudes $\theta_N = 80^\circ$ and $\theta_S = -80^\circ$ with periodic boundary conditions in the zonal direction. Furthermore the model uses restoring boundary conditions. Restoring the boundary at the surface of the oceanic basin to be a value based of a forcing field for Sea Surface Temperature (SST), Sea Surface Salinity (SSS), wind stresses (τ) and heat flux. The depth profile has 15 layers with grid stretching (figure 1). There are 90×40 grid points to make a $4^\circ \times 4^\circ$ resolution model.

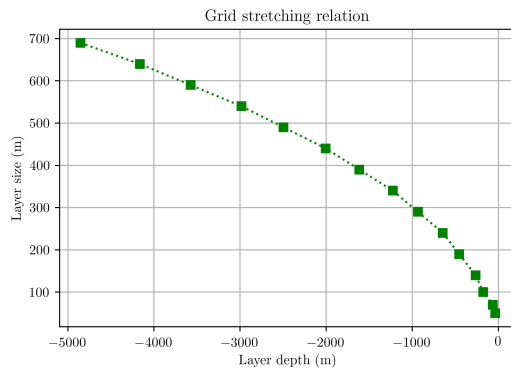


Figure 1: Grid stretching relation used

2.2.2 Surface Forcings

Choosing the correct forcing for the ocean is very important. It is known that the MOC in general circulation models is highly sensitive too even small

changes in surface forcings (Milliff et al. 1999). Attempts at making these forcings highly idealized have often been made in the past with varying rates of success. In this paper we will however use idealized forcings. Noting the fact, that this will probably induce the aforementioned errors in deep ocean circulations.

There were several methods that are explored when it comes to creating these idealized forcings. In the Mulder et al. 2017 paper an analytic forcing profile was used for wind flux, SST and SSS. This however fails to capture seasonal changes in each of the forcings due to the earths axial tilt. Something that can bring about a huge effect on the strength of the MOC. To combat this change a compromise is proposed. The SSS, SST and heat flux profiles are taken as zonal means for each month in the earths rotation. While the Zonal wind stress is set to the simple profile proposed by Bryan 1987. The analytic profile used in the paper is not specified specifically, but it can quite easily be deduced from the profile's plot. The choice of this analytic profile was made over a zonally averaged and equatorial averaged forcing $\mu(\tau_x)$. These were both tested on the present day configuration to see which of these forcings most accurately captures the present day MOC. In section 2.2.3 a comparison with the present day MOC and BSF is made.

2.2.3 MOC stream function

The global Meridional Overturning Circulation Ψ_{MOC} is defined as the zonally integrated meridional volume transport of water in the worlds oceans. It can be written down as:

$$\Psi_{MOC}(y, z) = \int_z^0 \int_{-180^\circ}^{180^\circ} v(x, y, z') dx dz'$$

Where v is the meridional component of the velocity. Ψ_{MOC} is thus a stream function of the zonally integrated volume transport in the Earth's water basins. Plotting this stream function can give a lot of insight into the deep water transport associated with the thermohaline circulation. In this paper we hope to capture these deep water transport formations as a

2.2.4 Barotropic Stream Function

It it furthermore interesting to look at an expression for the transport of ocean gyres. We know that

the depth integrated flow must be horizontally non-divergent. Thus a streamfunction Ψ_b can be introduced. Where $v(x, y, z)$ is the meridional velocity:

$$U = -\frac{\partial \Psi_b}{\partial y}; V = \frac{\partial \Psi_b}{\partial x} \quad (1)$$

$$\Psi_b = \int_{eastern bdy}^x \int_{-D}^0 v(x', y, z) dz dx' \quad (2)$$

Thus this so called barotropic stream function Ψ_b is defined by integrating the meridional transport westward from the eastern boundary of the domain. It is a useful tool to look at the shape and gyres associated with the major ocean current systems. By using the Sverdrup relation

$$\int_{-D}^0 v(x, y, z) dz = \frac{1}{\beta \rho_{ref}} \vec{z} \cdot \nabla \times \tau$$

first proposed by Sverdrup 1947 we can look at a schematic diagram of the barotropic stream function based on the prevailing zonal winds. figure 2 shows a schematic of this relation. It is easily visible how the prevailing zonal winds relate to the wind stress forcing seen in figure 3 on the next page. The calculation of the barotropic streamfunction without easily defined boundaries, is quite a complicated process done by Veros. (probably will add a discussion on this)

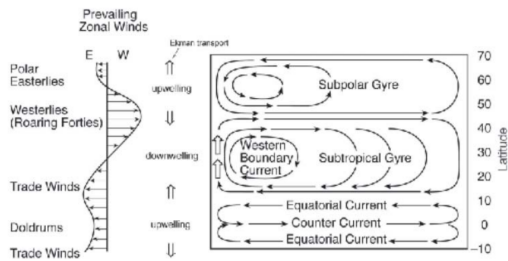


Figure 2: Schematic of the barotropic stream function based on the Sverdrup relation. Showing the subpolar and subtropical Gyres and equatorial currents. Figure taken from John Marshall 2012

2.2.5 Passage throughflow

For each of the passages mentioned in section 2.3 on the following page it is interesting to talk about the total volume transport through each of the passages. This is done using a simple integration to calculate the volumetric flux through each passage.

$$Q = \int \int_A \vec{u} \cdot d\vec{A} \quad (3)$$

For each passage a suitable location is chosen such that there are no boundaries next to the passageways, this is done for each time step. Then the u component of the flow is used to compute the total flow. This method is the same for each of the passages and thus we can study the effect of changes in bathymetry to on the relative strength of the flow. However, it should be noted that these values may not represent real physical values. As the passages in a 4° model are often only a few grid cells wide. Resulting in discrepancies in the calculation of the throughflow due to boundary conditions. There is however a more accurate way to calculate these throughflows. This can be done using the output of the Barotropic stream function discussed in section 2.2.4 on the previous page. This also gives us a measure of (purely zonal) throughflow in each grid cell. It is however difficult to get accurate values from this in Veros because the current version does not display the boundary values for the stream function.

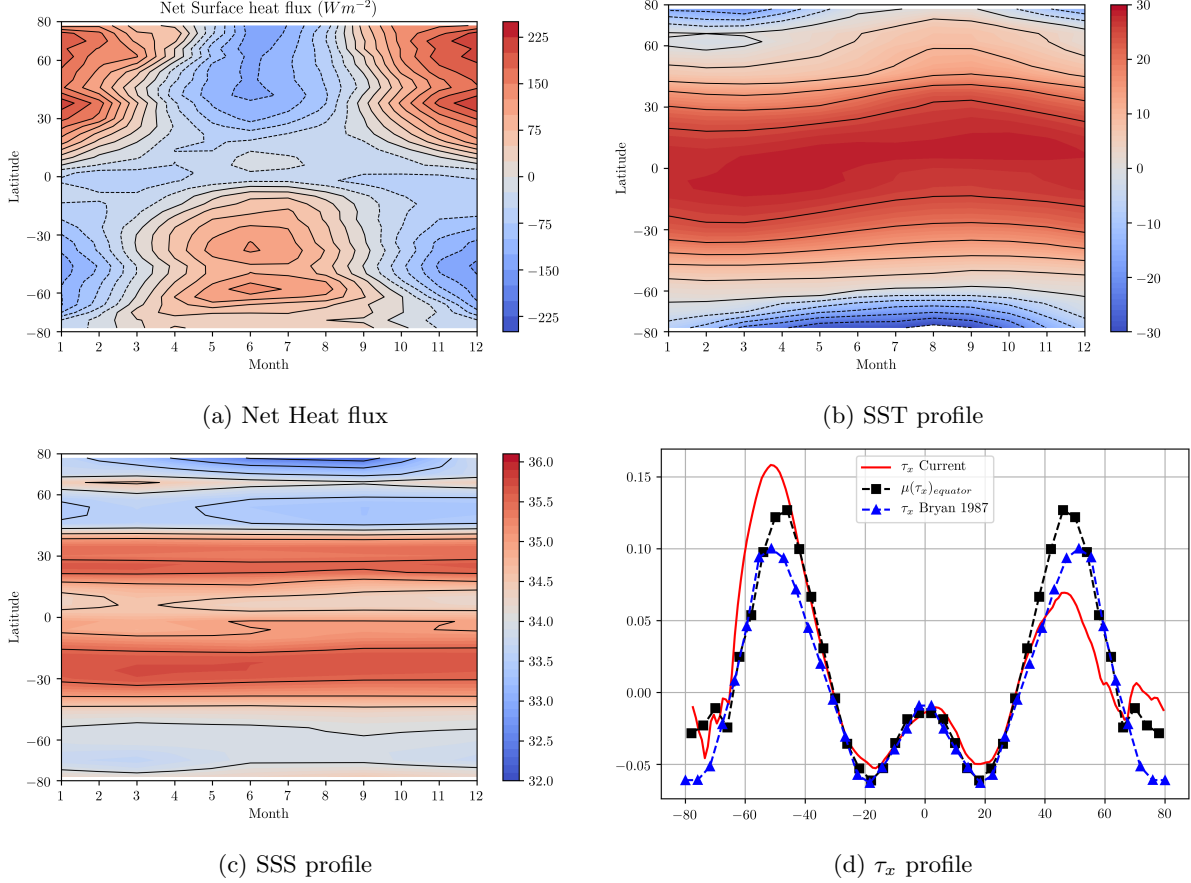


Figure 3: Idealized forcing profiles

2.3 Creating Bathymetries

To facilitate the model a set of 14 bathymetries were created in 5Ma time steps. These run from 65Ma to the present day configuration. These were reconstructed from bathymetries gained in Baatsen et al. 2016. These bathymetries were subsequently scaled to a 4 degree model and changed to address passage openings in the 4 degree case. Due to the low resolution of the model, choices have to be made with respect to the opening of certain passages. One of the choices that was made is that the northern Arctic sea is closed off in all of the bathymetries. This is mainly due to the fact that 4 degree models do not have enough resolution to facilitate this sea and Veros lacking the ability to have polar flow. The main events that shape the oceanic passages can be divided into time periods. These time periods are defined as follows in this paper. This deviates from their definitions in literature but serves only as a means of applying a name to the time steps.

	From	Until
Paleocene	65Ma	55Ma
Eocene	50Ma	35Ma
Oligocene	30Ma	20Ma
Miocene	15Ma	Present

2.3.1 Paleocene

In the paleocene a vast Pacific exists almost serving as a single basin. This period is largely characterized by the growth and development of a larger atlantic basin. Subsequently a decrease in size of the pacific basin is also seen. The drake passage is explicitly chosen to be closed in this time period, there is some evidence of it being opened in the paleocene due to a major change in the motion of the South American and Antarctic plates until about 50Ma (Livermore et al. 2005). However, the evidence proposes a shallow opening of less than 1 km in depth. These uncertainties and the extremely small nature of the basin has led to the decision to close the passage until its certain deep water con-

nection starting after the late Eocene as indicated by Livermore et al. 2005.

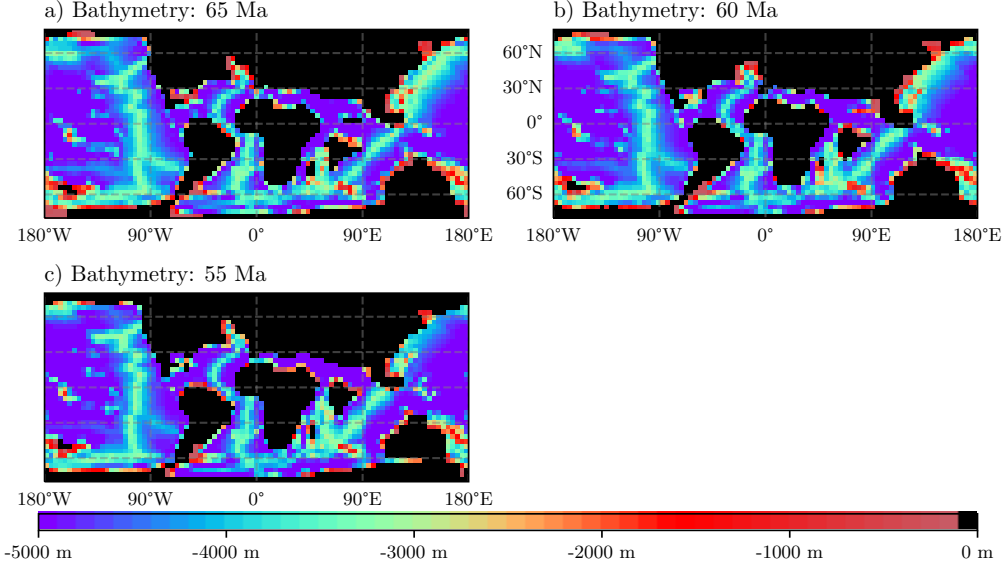


Figure 4: Paleocene Bathymetries showing **(a)** The bathymetry of 65 Ma. **(b)** The bathymetry of 60 Ma. **(c)** The bathymetry of 55 Ma

2.3.2 Eocene

The Eocene in contrast to the Paleocene is distinguished by the opening of certain passages connecting oceanic basins. These effects are often studied extensively for each individual passage in the literature. Choosing the exact timing for opening the passages is done manually by looking at often active research. The first of such passages to open is the Tasman passage which is opened at 35 Ma

as a shallow passage slowly growing in size (Lawer and Gahagan 2003). The Tasman passage opening is believed to have had a large impact on the onset of the Atlantic circumpolar current (ACC). From the onset of the early Eocene the Indian Continent has been fast moving towards the north slowly closing the northern passage between the Indian ocean and the Tethys seaway. The water passage is closed from 35 Ma based on Najman et al. 2010.

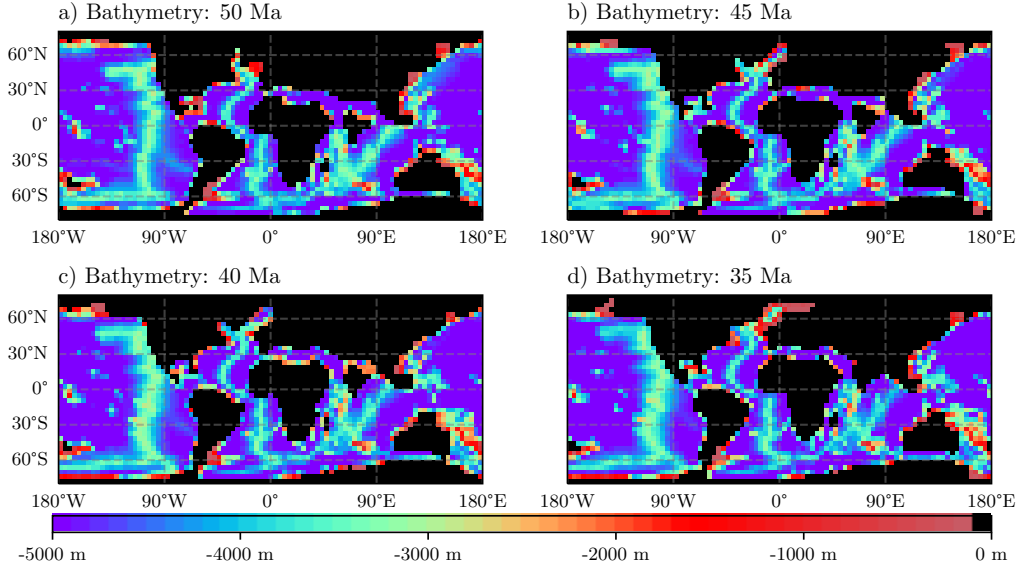


Figure 5: Eocene Bathymetries showing (a) The bathymetry of 50 Ma. (b) The bathymetry of 45 Ma. (c) The bathymetry of 40 Ma.(d) The bathymetry of 35 Ma

2.3.3 Oligocene

From the onset of the Oligocene The Total circulation of water around the Antarctic basin is finalized by the opening of the shallow Drake passage at around 30Ma. 30Ma is specifically chosen to differentiate between the opening of the drake and Tasman passages. Especially since there is still

some debate on the exact timing of drake passage opening (Scher and Martin 2006; Livermore et al. 2005). These openings coincide with the onset of the Antarctic circumpolar current that has had major effects on the global climate variability. Furthermore, The Oligocene is characterized by the further expansion of the Atlantic basin and a Tethys seaway that is becoming more shallow.

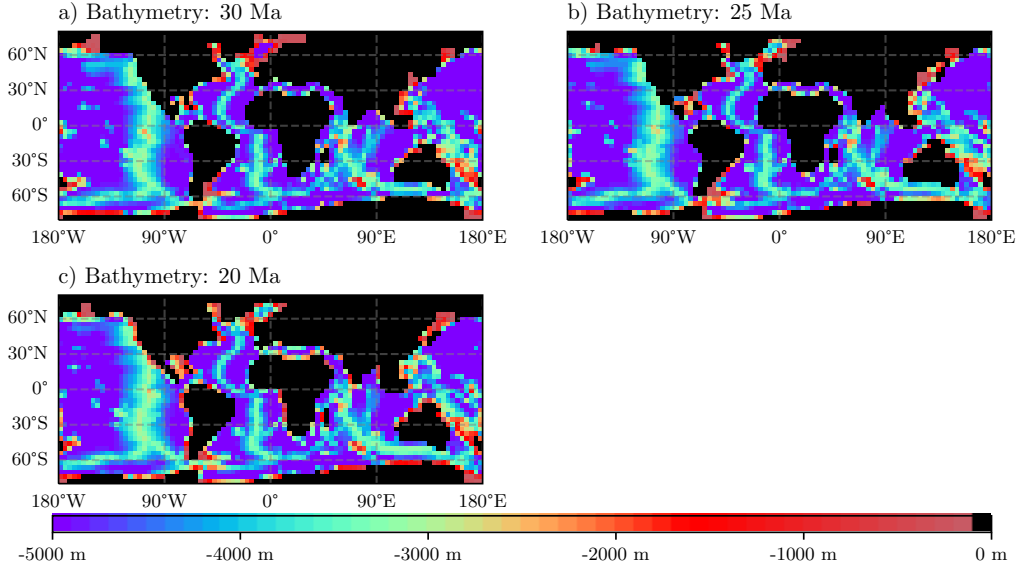


Figure 6: Oligocene bathymetries showing: (a) The bathymetry of 30 Ma. (b) The bathymetry of 25 Ma. (c) The bathymetry of 20 Ma.

2.3.4 Miocene

The Miocene is characterized by some more passage closures. The Tethys seaway had been decreasing in size in the previous 20 Ma. It finally fully detaches the Mediterranean sea to the Indian ocean

from 15 Ma onward (Hamon et al. 2013). Then another major change occurs with the closure of the Panama seaway from 5 Ma onward (Molnar 2008; Pindell et al. 1988). Stopping the mid latitude throughflow between the Atlantic and Pacific basins.

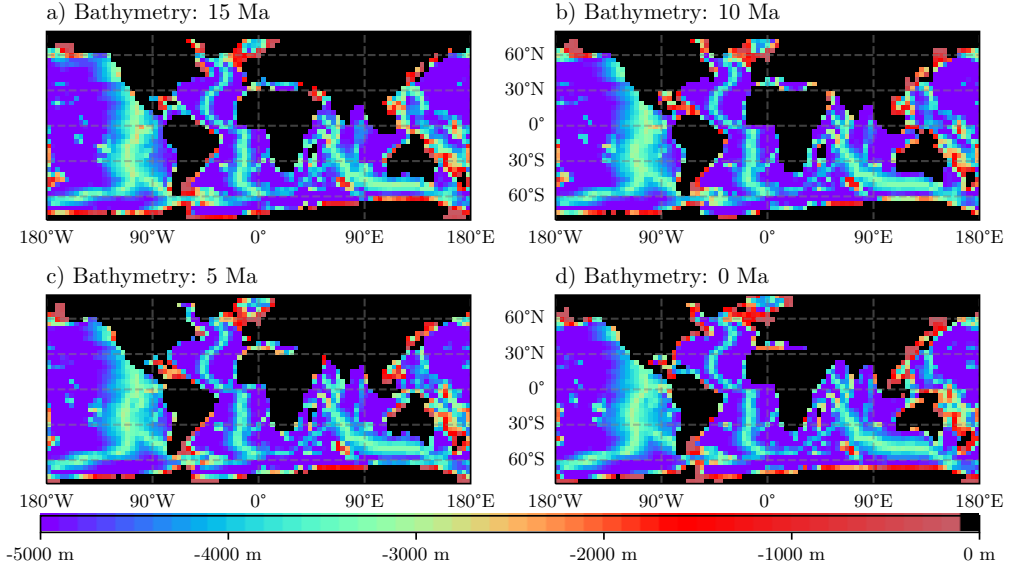


Figure 7: Miocene bathymetries showing (a) The bathymetry of 15 Ma. (b) The bathymetry of 10 Ma. (c) The bathymetry of 5 Ma.(d) The present day bathymetry

3 Results

3.1 Model Quality

To assess the quality of the model and thus if any of the results resemble reality, one can compare the present day setup of the model to an existing model with realistic forcings. Also, the model can be compared to a higher resolution model. This is done to check how good the model is and whether any of the results have any connection to reality.

3.1.1 Quality of BSF

To look at the quality of the barotropic stream function we compare the barotropic stream function of our model to a 4° model with realistic forc-

ings. This model was made with the standard Veros setup with custom open Indonesian passage. In figure 8 on the following page we see that the barotropic stream function itself is remarkably similar. Only showing a weaker subtropical gyre in the Indian ocean and a weaker gulf stream. In the temperature profile at 245 meters in depth there are however larger discrepancies. There is a 4°C difference in temperature in the gulf stream and a 2°C temperature difference in the Kuroshio gyre. This can be attributed to weaker SST forcing at the surface on these places because of the zonal mean nature of these forcings and also due to the shorter runlength of the model. Thus the model did not yet get adequate time to fully develop the flows (THIS COULD BE BETTER)

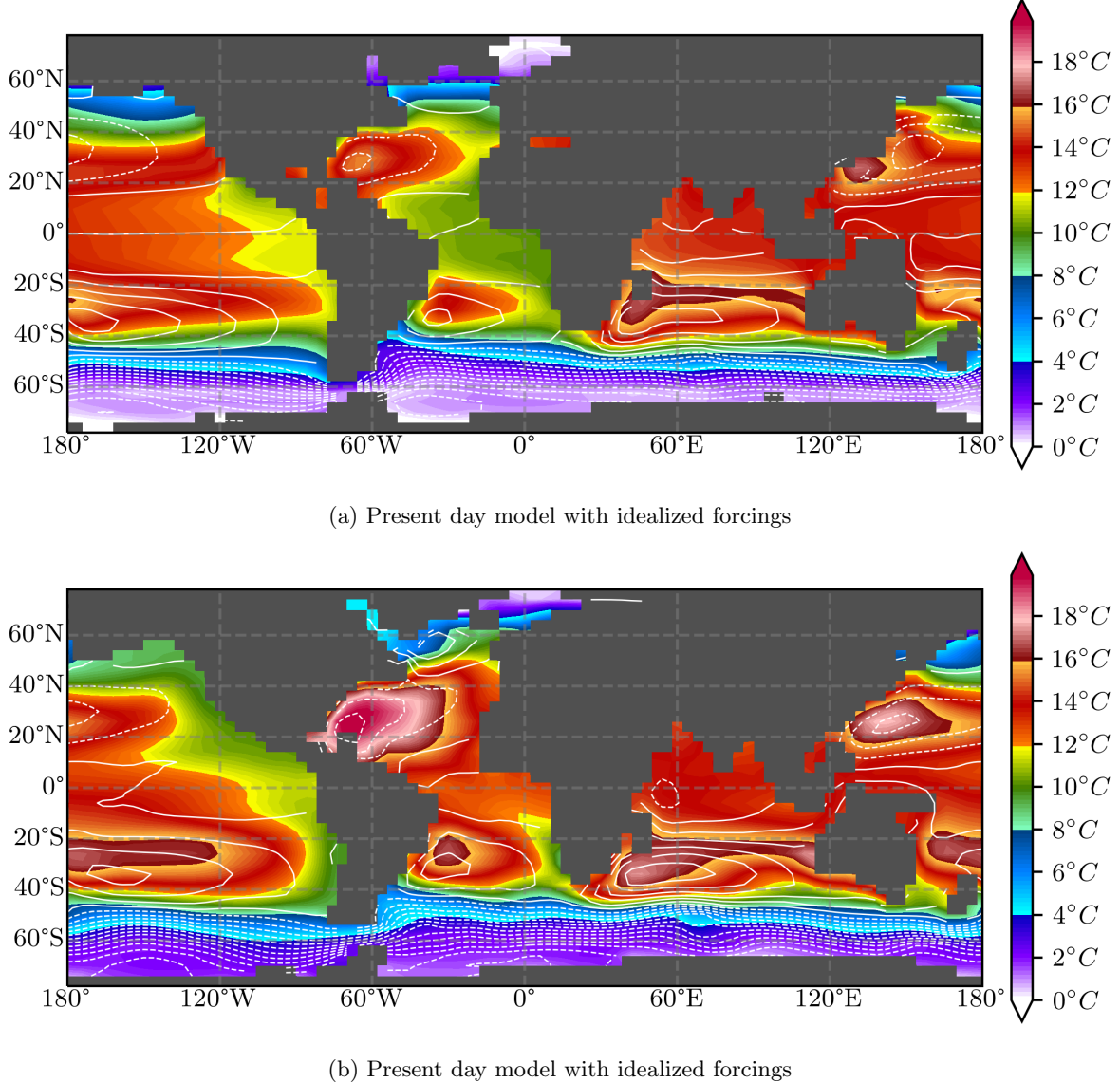


Figure 8: Figures comparing the Barotropic stream function (contours) and temperature at 245m depth of **a**) an idealized model and **b**) a model with realistic forcings

3.2 Passage throughflow

As discussed in section 2.2.5 on page 3 the passage throughflow can be calculated using the velocity field for each time step. To do this a suitable location was chosen for each time step and passage such that there are no boundaries next to the passageways. This method is the same for each of the passages, noting that only zonal flow was studied. Thus we can study the effect of changes in bathymetry to on the relative strength of the flow. The passageways have been labeled in figure (figure

of these). The computed throughflow can be seen in figure 9 on the following page. In this figure the onset of the ACC is clearly visible. Showing that due to the northward movement of Australia and the deepening of the drake passage the total volume transported by the ACC grows dramatically over time. Furthermore it can be seen that the closure of the drake passage causes the flow through the aghulas passage to reverse in direction. Furthermore, the throughflow through the panama passage is shown to slow due to both the onset of the ACC and the closure of the thetys seaway. Finally re-

versing the direction of flow through the panama passage at 15Ma due to the total closure of the thetys sea. The reversal of the Indonesian through-flow observed by Mulder et al. 2017 is not observed with total throughflow always moving water east to west. This is however in agreement to the flow found by Omta and Dijkstra 2003 in a shallow water model. Note however, that the land masks used by them are different to the land masks used in this paper.

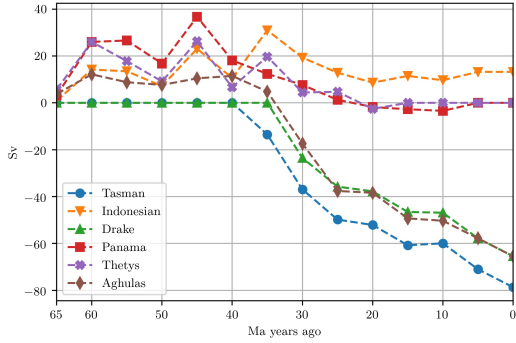


Figure 9: Total volume transport in Sverdups for 7 passages. Running from 65 milion years ago to the present day situation. Positive values indicate transport to the west

Rather than looking only at volume transport in the upper layers the transport can also be split into a deep water transport layer ($< -2000m$) and a surface transport layer($> -2000m$). Doing this gives insight into the thermohaline circulation. In the deep water transport layer seen in figure 10 we see a very diffrent picture to the total volume transport. It is however hard to draw any conclusions from this image. It is only 6 integration layers deep and fluctuations in the depth of each passage accounts for most of the differences comparing each time step.

To get an even better understanding of the flows, we can look at a vector field showing the direction of horizontal water displacement for each of the time steps. This is done by making a weighted mean of the horizontal flow field for each layer. Weighted by the volume of each grid cell. In this way each arrow actually represents relative flow velocity compared to other grid points. Thus showing

the velocity field of the ocean.

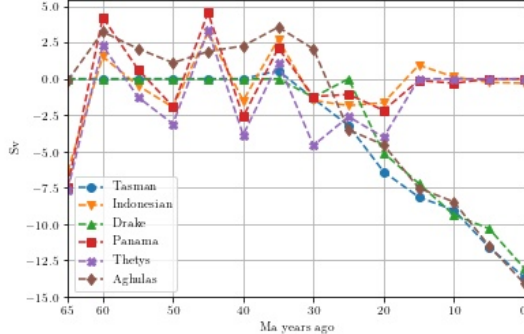
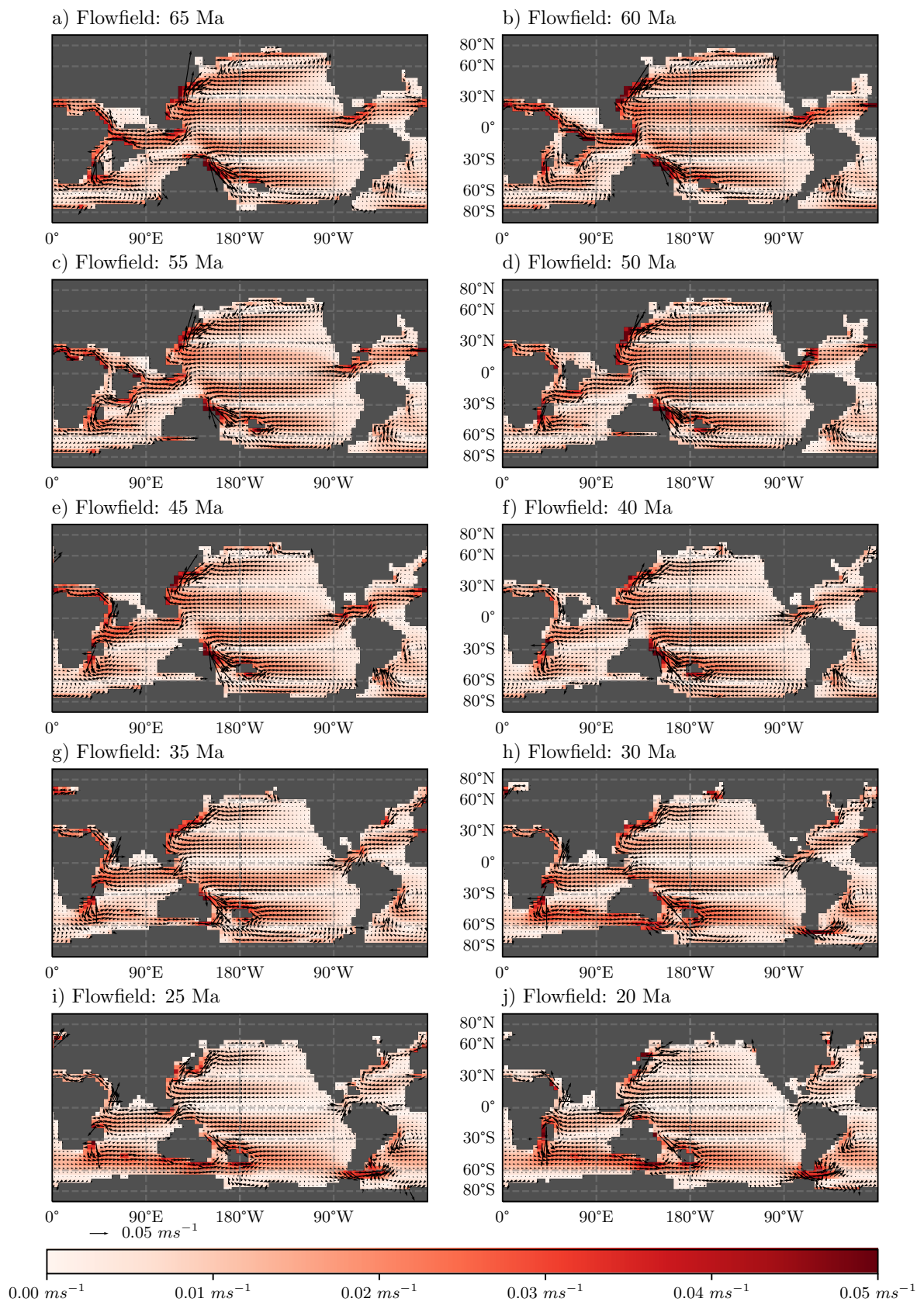


Figure 10: Total volume transport in the deep water layer ($< -2000m$) in Sverdups for 7 passages. Running from 65 milion years ago to the present day situation. Positive values indicate transport to the west

This field is shown in figure 11 on page 13. Here the ACC is very noticible. The reversal of flow through the panama passage at 15Ma is the most interesting result here. Where here we find the closure of the Thetys seaway to be the main factor. However, the reversal only occurs after the closure of the seaway. This is in contrast to the results obtained by Omta and Dijkstra 2003 where the flow reversal was observed to coincide with the opening of the drake passage. Here we only observe a decease in volume transported through the passage, but no such reversal until the Thetys seaway is closed.

The largest changes in the flow field are observed in the Indian ocean. The indian continent moves northward at a very fast pace. After 55 Ma the flow through the passage north of the Indian continent is massively reduced and instead the water flows east of the continent into the thetys seaway. No "circum India" current is observed in any of the time steps. The position of the Indian continent does however seem to have a strong influence on the strength of the Aghulas sub-tropical gyre. This can probably be explained by the amount of water that is transported through the Tethys seaway. There being a large fluctuation in the strength of the gyre. The size of this gyre also increases with time due to this northward movement.



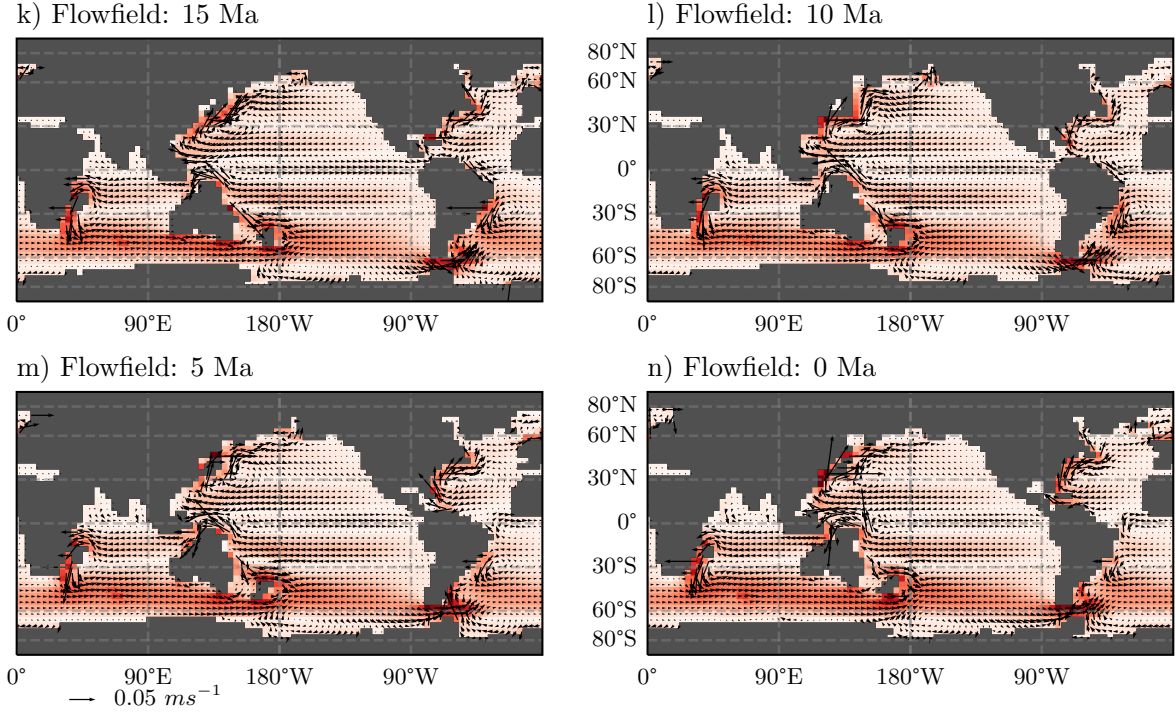


Figure 11: Flow field

3.3 Barotropic Stream function

Next we will look at the barotropic stream function for each of the time steps discussed here. Some of the flows that are discussed in this section are closely related to the flows explained in section 3.2 on page 9. Here we will have a stronger focus on the flows gyres seen in the ocean and their relative strength in a time sense. Each of the oceanic basins is discussed in detail. An overview of each of the barotropic stream functions can be seen in figure 13 on page 17. It is very visible that the boundary conditions of the BSF are not shown here. This is due to the previously stated fact that they are excluded from the model output produced by Veros.

It must however be noted that this does not mean that flows through the passages are not modeled but rather only that the passages themselves do not show up on the plots of the barotropic stream function. In this case the barotropic stream function serves only to see the major ocean gyres and how water is transported in these gyres.

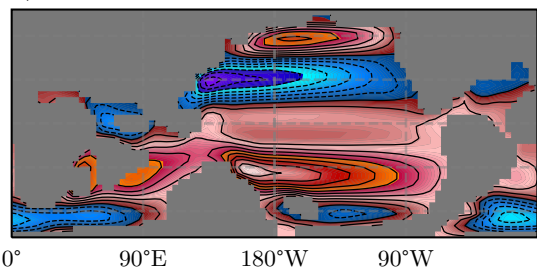
3.3.1 Indian Ocean

3.3.2 Pacific Ocean

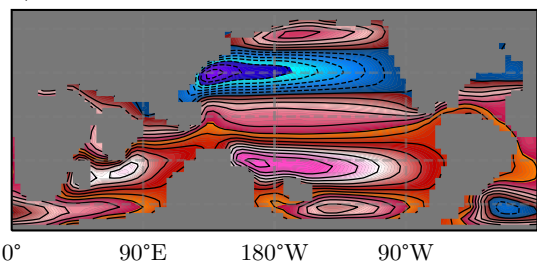
The pacific ocean is of particular interest in this case. It is easily vi

3.3.3 Atlantic Ocean

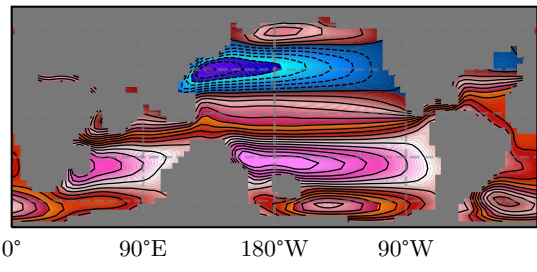
a) BSF: 65 Ma



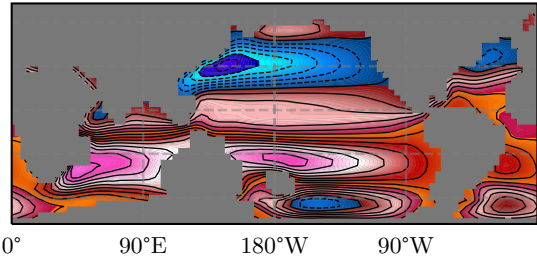
c) BSF: 55 Ma



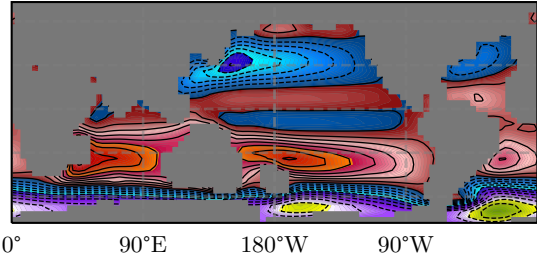
e) BSF: 45 Ma



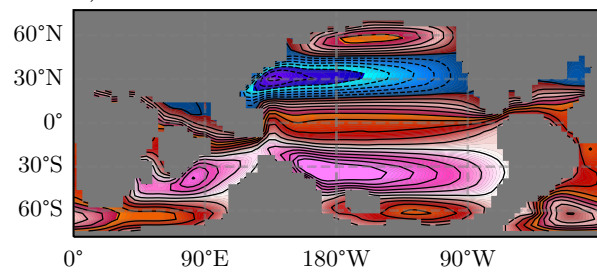
g) BSF: 35 Ma



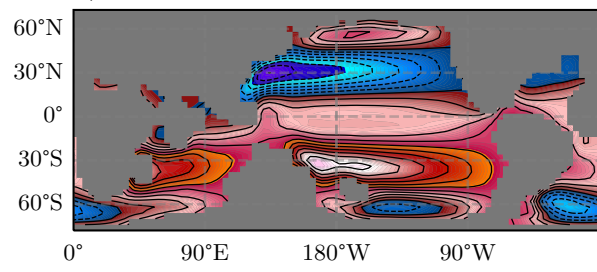
i) BSF: 25 Ma



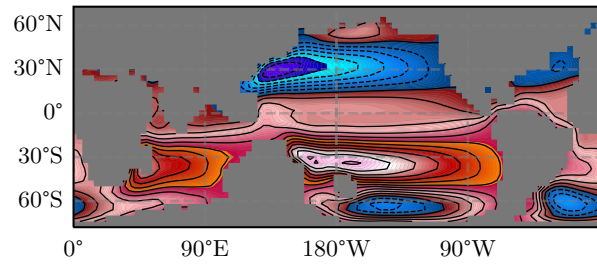
b) BSF: 60 Ma



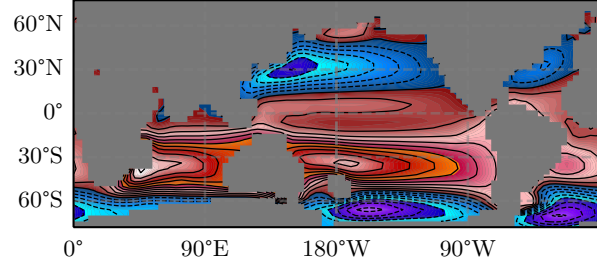
d) BSF: 50 Ma



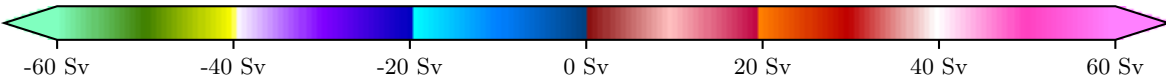
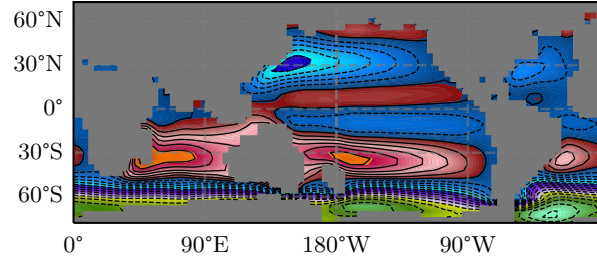
f) BSF: 40 Ma



h) BSF: 30 Ma



j) BSF: 20 Ma



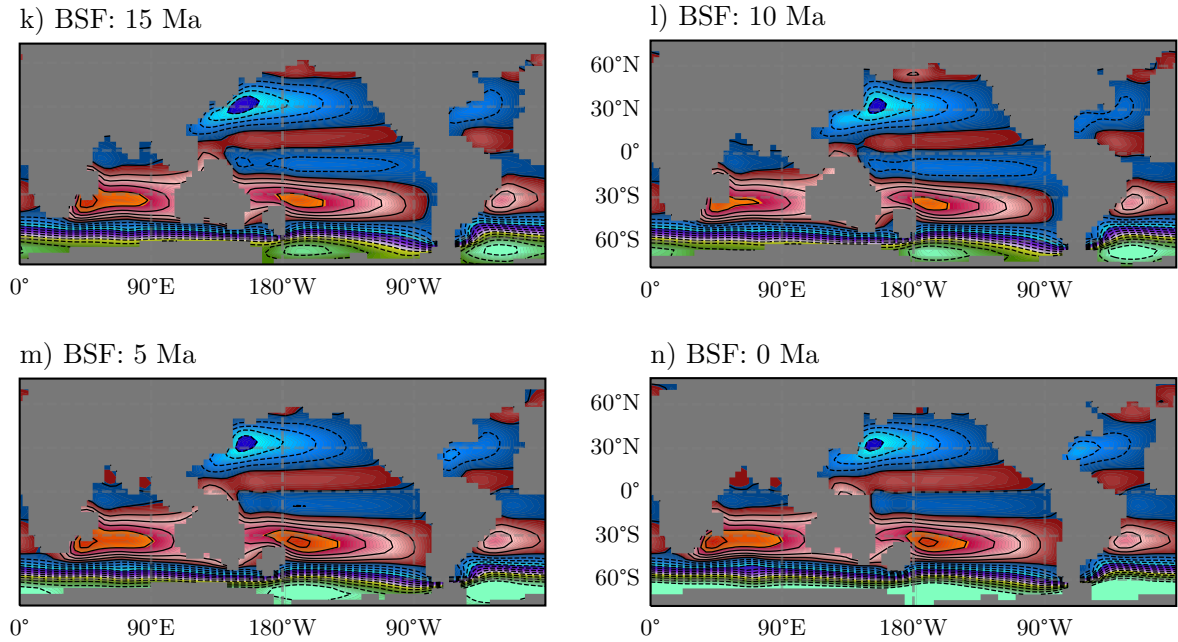
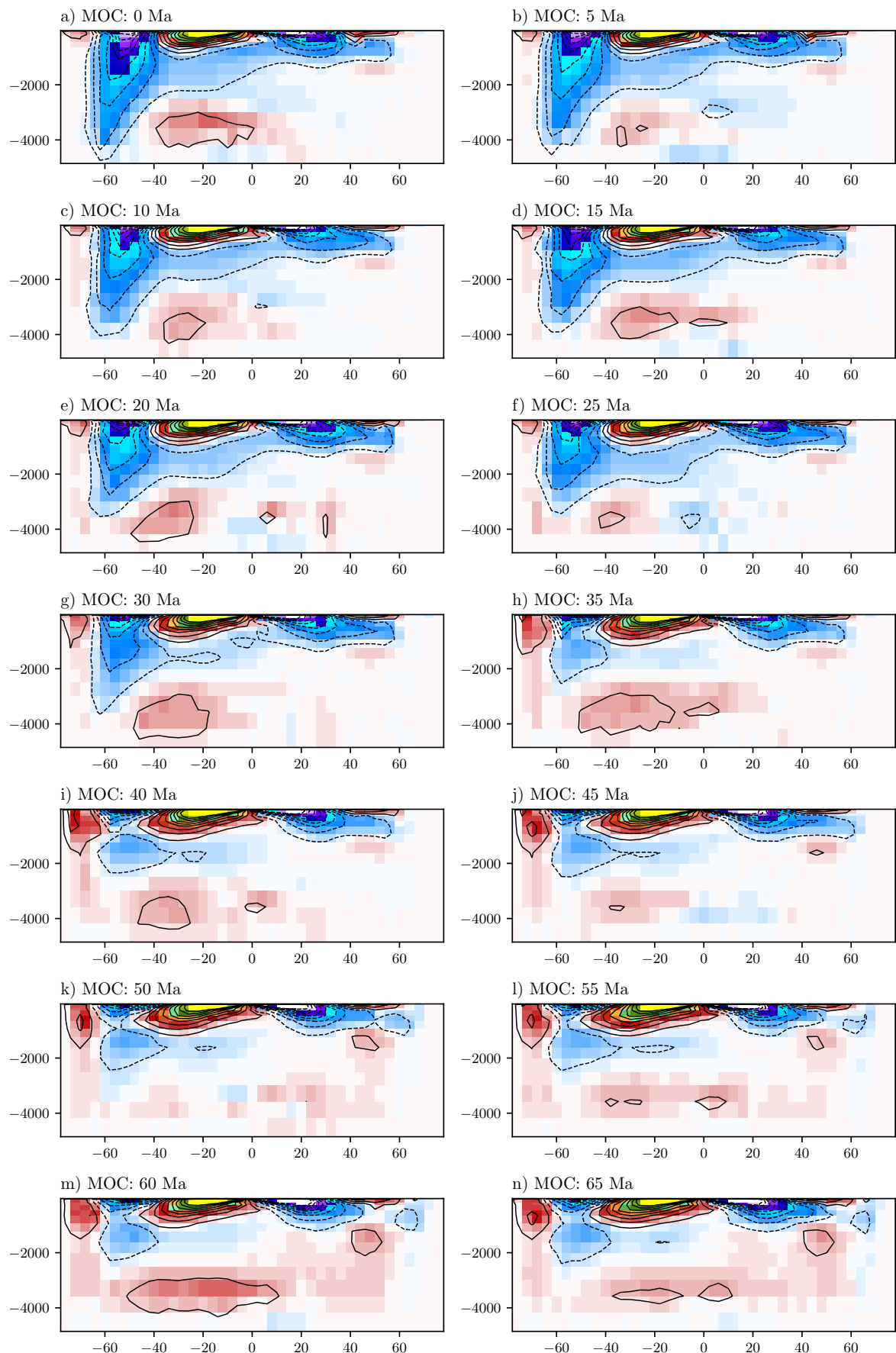


Figure 12: Barotropic Stream Function with contour lines every $5Sv$

3.4 MOC Stream function

The meridional overturning circulation (MOC) is characterized by large changes in the



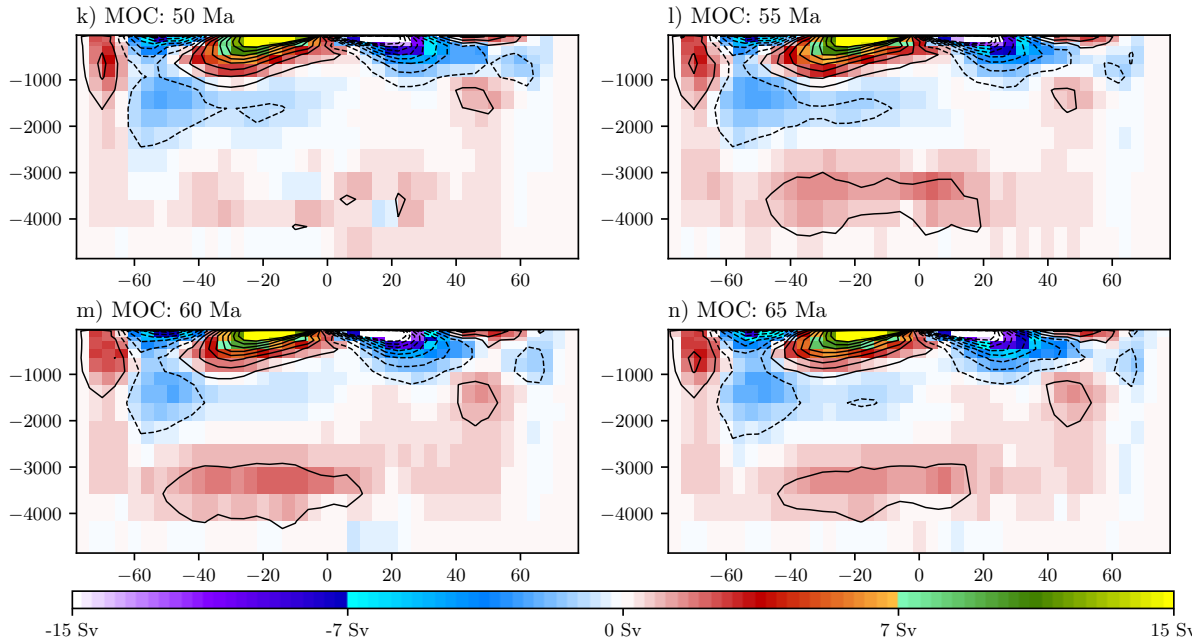


Figure 13: Barotropic Stream Function

4 Summary

0/100 done

5 Discussion

- Discuss the results and flaws in these.
 - Discuss possible future research.
 - Discuss possible improvements.
 - Discuss possible 1 degree models.
 - Discuss troubles with the ACC strength due to the forcings.
 - Discuss the difficulty with trial and error in the model.
 - Discuss Climate changes and their major effects that have been ignored.
 - Discuss what can be concluded from these results.
- 0/100 done

References

- [1] Jean Besse and Vincent Courtillot. "Apparent and true polar wander and the geometry of the geomagnetic field over the last 200 Myr". In: *Journal of Geophysical Research: Solid Earth* 107.B11 (2002), EPM-6.
- [2] Howie D. Scher and Ellen E. Martin. "Timing and Climatic Consequences of the Opening of Drake Passage". In: *Science* 312.5772 (2006), pp. 428–430. ISSN: 0036-8075. DOI: 10.1126/science.1120044.
- [3] D. N. Schmidt. "The closure history of the Panama Isthmus: Evidence from isotopes and fossils to models and molecules". In: *ResearchGate* (2007), p. 429444. URL: https://www.researchgate.net/publication/282323290_The_closure_history_of_the_Panama_Isthmus_Evidence_from_isotopes_and_fossils_to_models_and_molecules.
- [4] Meir Abelson and Jonathan Erez. "The onset of modern-like Atlantic meridional overturning circulation at the Eocene-Oligocene transition: Evidence, causes, and possible implications for global cooling". In: *Geochemistry Geophysics Geosystems* 18 (May 2017). DOI: 10.1002/2017GC006826.
- [5] T. E. Mulder et al. "Efficient computation of past global ocean circulation patterns using continuation in paleobathymetry". In: *Ocean Modell.* 115 (2017), pp. 77–85. ISSN: 1463-5003. DOI: 10.1016/j.ocemod.2017.05.010.

- [6] Ralph F. Milliff et al. "Ocean general circulation model sensitivity to forcing from scatterometer winds". In: *J. Geophys. Res. Oceans* 104.C5 (1999), pp. 11337–11358. ISSN: 0148-0227. DOI: 10.1029/1998JC900045.
- [7] Frank Bryan. "Parameter sensitivity of primitive equation ocean general circulation models". In: *Journal of Physical Oceanography* 17.7 (1987), pp. 970–985.
- [8] Harald Ulrich Sverdrup. "Wind-driven currents in a baroclinic ocean; with application to the equatorial currents of the eastern Pacific". In: *Proceedings of the National Academy of Sciences of the United States of America* 33.11 (1947), p. 318.
- [9] R. Alan Plumb John Marshall. "Atmosphere, Ocean and Climate Dynamics: An Introductory Text". In: San Diego, California: Elsevier Academic Press, 2012. Chap. The wind-driven circulation, p. 214. ISBN: 978-0125586917.
- [10] Michiel Baatsen et al. "Reconstructing geographical boundary conditions for palaeoclimate modelling during the Cenozoic". In: *Clim. Past* 12.8 (2016), pp. 1635–1644. ISSN: 1814-9324. DOI: 10.5194/cp-12-1635-2016.
- [11] Roy Livermore et al. "Paleogene opening of Drake Passage". In: *Earth Planet. Sci. Lett.* 236.1 (2005), pp. 459–470. ISSN: 0012-821X. DOI: 10.1016/j.epsl.2005.03.027.
- [12] Lawrence A. Lawver and Lisa M. Gahagan. "Evolution of Cenozoic seaways in the circum-Antarctic region". In: *Palaeogeogr. Palaeoclimatol. Palaeoecol.* 198.1 (2003), pp. 11–37. ISSN: 0031-0182. DOI: 10.1016/S0031-0182(03)00392-4.
- [13] Yani Najman et al. "Timing of India-Asia collision: Geological, biostratigraphic, and palaeomagnetic constraints". In: *J. Geophys. Res. Solid Earth* 115.B12 (2010). ISSN: 0148-0227. DOI: 10.1029/2010JB007673.
- [14] N. Hamon et al. "The role of eastern Tethys seaway closure in the Middle Miocene Climatic Transition (ca. 14 Ma)". In: *Clim. Past* 9.6 (2013), pp. 2687–2702. ISSN: 1814-9332. DOI: 10.5194/cp-9-2687-2013.
- [15] Peter Molnar. "Closing of the Central American Seaway and the Ice Age: A critical review". In: *Paleoceanography* 23.2 (2008). ISSN: 0883-8305. DOI: 10.1029/2007PA001574.
- [16] James L. Pindell et al. "A plate-kinematic framework for models of Caribbean evolution". In: *Tectonophysics* 155.1 (1988), pp. 121–138. ISSN: 0040-1951. DOI: 10.1016/0040-1951(88)90262-4.
- [17] Anne Willem Omata and Henk A Dijkstra. "A physical mechanism for the Atlantic-Pacific flow reversal in the early Miocene". In: *Global and planetary Change* 36.4 (2003), pp. 265–276.